Desalination and Water Treatment
www.deswater.com

doi:10.5004/dwt.2017.21802

100 (2017) 193–203
December

Removal of Cd by humic acid modified TiO_2 nanoparticles from aqueous solution

Shamshad Khan[a], Zhang Dan[a,*], Yang Mengling[a,b], Yang Yang[c], He Haiyan[a,b], Jiang Hao[a]

[a]*Key Laboratory of Mountain Environmental Diversity and Control, Institute of Mountain Hazards and Environment, Chinese Academy of Sciences and Ministry of Water Conservancy, Chengdu 610041, China, email: shamshadkhan768@yahoo.com (S. Khan), Tel. +86 13708008342, Fax +86 28 85222258, email: daniezhang@imde.ac.cn (D. Zhang), 457638428@qq.com (Y. Mengling), 298989633@qq.com (Y. Yang), 429602425@qq.com (H. Haiyan), jianhao@imde.ae.cn (J. Hao)*
[b]*University of Chinese Academy of Sciences, Beijing 100081, China*
[c]*Yibin Branch Company, Sichuan Tobacco Company, Yibin 644000, China*

Received 17 July 2017; Accepted 10 December 2017

ABSTRACT

In this study, removal of Cd from aqueous media by the adsorption of TiO_2 nanoparticles (TNPs), with surface modification by humic acid (HA) was assessed. Results showed a linear increase of the coating percentage from 100–HA to 250–HA but no significant difference between the HA coated TNPs prepared at 250 and 350 mg L^{-1} due to an extremely narrow band gap. The obtained materials (HA–TNPs) were characterized by Fourier transform infrared spectroscopy and UV–visible spectrophotometer. Then, batch adsorption techniques were carried out to examine the possible adsorption mechanisms of Cd onto TNPs and HA–TNPs. It was noted that the adsorption capacity of the HA–TNPs for Cd enhanced considerably as compared to that of the bare TNPs, implying that HA coating might modify bioavailability of Cd in aquatic environment. Equilibrium data were best described by the Freundlich equation, and the partition distribution coefficient (k) of HA–TNPs increased by 34%, 50% and 59% for Cd at 298, 315 and 332 K respectively, as compared to the bare TNPs, suggesting that HA–TNPs had a stronger affinity of sites for Cd adsorption than that of bare TNPs.

Keywords: TiO_2 nanoparticles; Surface modification; Cadmium; Adsorption capacity

1. Introduction

Heavy metals are some of the mainly serious environmental pollutants in water and soil. Heavy metal pollution poses a risk to the environment, and it can be harmful to human health via the food chain. Strict environmental regulations on the discharge of heavy metals and increasing demands for clean water with low levels of heavy metals make it greatly significant to develop a variety of efficient technologies for heavy metals removal [1–4]. However, various common methods to remove heavy metals from wastewater including reduction and precipitation, coagulation and flotation, ion exchange, membrane technology, and electrolysis are generally expensive or ineffective, particularly when the metal concentration exceeds 100 ppm [5]. These disadvantages have increased the need to develop alternative and low-cost water treatment methods for heavy metals [6].

The development in the field of science and engineering propose that several of the existing problems involving water quality could be resolved or reduced utilizing nanotechnology [7]. Considerable attention has been given to the development of nanomaterials absorbents with increased adsorption rate, capacity, selectivity for the target metals, various adsorbents such as carbon nanotube [8], nanosized zero-valent iron [9], nanoscale zero-valent manganese [10], nanosized metal oxides [11] have been investigated for the removal of heavy metals. The large surface areas, well-defined pore sizes, high pore volume and high adsorption capacity, ease of modification, and diversity in surface functionalization of nanomaterials absorbents can give extraordinary chances for the adsorption of heavy metals in highly efficient and cost-effective approaches [12]. It was reported

*Corresponding author.

that modification/functionalization of nanoparticles surfaces generate the binding capacities for heavy metals and provide the dispersion stability in suspension medium [12]. Recently, much consideration has been given on surface modification of nanomaterials absorbents by utilizing glycine, chitosan, gum arabic, glutaralde-hyde, polyethylenimine, polyer, EDTA, amino groups, 3-mercaptopropionic acid , citric acid, poly(acrylic acid), and humic acid etc. [13]. However, most of these nanomaterials absorbents and their surface modification/functionalization process experience from high cost and/or the utilization of some environmentally incompatible additives;therefore the application of above mentioned nanomaterials may cause potential environmental hazards [14]. Consequently, the development of low-cost, environmental-friendly and biocompatible nanomaterial-based adsorbent is required for heavy metals removal.

The application of TNPs as biocompatible adsorbent [15] for the adsorption and immobilization of heavy metals has gained importance in view of its particular chemical composition and crystal structure [16]. TNPs are widely used in hard tissue replacement because of its nontoxicity and biocompatibility [15], and have been considered as an environmental benign functional material with remarkable capacity to absorb heavy metals [16]. Furthermore, TNPs most commonly used semiconductors photocatalyst since they are highly photoactive, photostable, biologically and bio-chemically inert and relatively inexpensive. The photochemical technology using TNPs photocatalyst for the water treatment process is known as a clean method. It is now well established that the photocatalytic activity of TNPs generally depends on its morphology, crystal composition, crystallinity, particle size, surface area and porosity [17–20]. At present, TNPs have attracted a great deal of attention due to its very favorable ligand sorption properties through inner sphere complex formation [21] for removal of organic contaminants; others suggest this is due to electrostatic interaction and hydrogen bonding between TNPs and organic polar side groups [22]. In addition, it has been reported that there is no significant phytotoxicity of TNPs were observed through a seed germination test of lettuce [23], while TNPs have been used as nanoscale amendments in agriculture due to their photocatalytic properties. TNPs inhibit pathogenic infection in cucumber by Pseudomonas syringae pv. lachrymals (68.6%) and P. cubensis (90.6%) [24]; importantly, the authors also reported significant increases in photosynthetic activity (30%) as compared to control plants. Therefore, TNPs exhibit great potential to be used as biocompatible and environmental-friendly adsorbents for heavy metals removal from aqueous media.

Till date, numerous magnetic nanomaterials, including maghaemite nanoparticles [25], Fe_3O_4 magnetic nanoparticles [26], Fe_3O_4 nanoparticles functionalized and stabilized with compounds like humic acid, amino-functionalized polyacrylic acid (PAA) [27], and different biopolymers like gum arabic [28], chitosan [29] and polysaccharides [30] have been explored for the removal of heavy metals. Based on the above results, we can conclude that the compounds used for the surface modification or functionalization of adsorbents have some what significant in common, such as; these compounds show strong metal complexing ability. Keeping this in view, more and more researchers are experimenting to come up with better alternatives to the existing options [31,32]. Aquatic humic acid (HA) constitutes 30–50% of NOM in natural aquatic systems [33]. Humic acid (HA) has a skeleton of alkyl and aromatic units that attach with carboxylic acid, phenolic hydroxyl, and quinone functional groups [34]. As these functional groups have high complex ability with heavy metal ions, humic acid (HA) was applied to remove heavy metal ions from water. Binding of humic acid (HA) to nanomaterials influences the sorption behavior of both humic acid (HA) and nanomaterials [13]. This is because the adsorption of humic acid (HA) results in a polyanionic organic coating on nanomaterials and thus essentially altering the surface properties of the particles [13]. Enhanced removal of heavy metals through HA modification/coating of Fe_3O_4 magnetic nanoparticles have been examined before [35,36]. In addition, HA could also coaton the surface of carbon nanotubes, graphene oxide nanosheets, SiO_2, TiO_2, Al_2O_3or ZnO nanoparticles, making removal of atrazine [37], phenanthrene [38], ionizable aromatic compounds [39] and heavy metals [40] more effective from aqueous media. However, as for the biocompatible TNPs, little information is available regarding the mechanisms between TNPs and humic acid. Alternately, the possibility of using humic acid modified TNPs as an adsorbent material to remove heavy metals from wastewater is however not explored. In our previous work, organic matter has been proven to have great binding affinities for TNPs surface [34]. And thus, according to above introduction, humic acid modified TNPs may be a potential adsorbent for removal of heavy metals from aqueous solution.

In the present work, a novel biocompatible and environmental-friendly nanostructured absorbent prepared by modifying TNPs with HA (denoted as HA–TNPs) has been tested for the removal of Cd from aqueous media. The physical and chemical characterization of the prepared HA modified TNPs were carried out, and the applicability of HA–TNPs in Cd removal was estimated in view of the adsorption kinetic and capacity, as well as effects of pH and temperature.

2. Materials and methods

2.1. Materials and chemicals

TiO_2 nanoparticles (anatase from) and humic acid were purchased from Sigma-Aldrich (Ankara, Turkey). TNPs have purity, diameter, and specific surface area of 99.7%, 25 nm, and 45–55 m^2/g, respectively. The pH_{ZPC} (zero point of charge) of TNPs is approximately 4.2 determined by Zetasizer Nano S Instrument (Malvern Instrument Ltd, Malvern) as described in detail in our previous work [30] and humic acid (>99%) is black crystalline powder, which is selected as a NOM model molecular used in this study. Total organic carbon analyzer (Apollo 9000, Teledyne Tekmar), was used to determine the TOC content of HA, after centrifuging and filtering through disposable 0.45-µm membranes. Cd solution was prepared from of cadmium ($Cd(NO_3)_2{\cdot}4H_2O$) (purity >99%). All other solutions were prepared using analytical grade chemicals (National Medicine Corporation Ltd., Shanghai, China) and Milli-Q element ultrapure water (18.2 X, Millipore, Billerica, MA, USA). All the glassware was prewashed with 5% HNO_3 for 24 h, systematically rinsed with distilled water and Milli-Q water three times, respectively, and dried at 60°C before use.

2.2. Preparation of modified TNPs with humic acid (HA)

The steps of preparation of HA coated TNPs followed the previous description of Yang and Xing [38] with minor modifications. Briefly, 5 g TNPs was mixed with 1 L HA solution in a bottle and shaken for 2 d, after which the suspensions were centrifuged at 3500 *g* for 30 min. The precipitated materials were freeze-dried, ground, and stored for future experiments. HA concentrations in solution were 100, 250, and 350 mg L^{-1} for TNPs. The residual HA concentrations in solution after coating were measured by total organic carbon (TOC) analysis (Shimadzu, TOC-VCPH). The carbon contents of TNPs, and modified TNPs with HA (HA–TNPs) were determined using an elemental analyzer. These samples and HA were also characterized by Fourier transform infrared (FTIR) spectroscopy and UV–visible spectrophotometer. HA modified TNPs were labeled by the HA concentrations. For example, 100–HA–TNPs represented the TNPs modified by 100 mg L^{-1} of HA.

2.3. Adsorbent characterization

Preliminary experiments were done to estimate the necessary time required to obtain equilibrium for Cd adsorption by the TNPs or HA–TNPs, which could be attained after 2 h as shown in Fig. 3A. Therefore, an equilibrium time of 2 h was selected in this study. Adsorption experiments were performed by shaking a certain amount of TNPs or HA–TNPs adsorbent with 50 mL of the aqueous solution of Cd in various 50 mL polyethylene centrifuge using a temperature-controlled shaker. The pH of the solutions was adjusted with HNO_3 or NaOH and was determined both before and after each experiment. The TNPs or HA–TNPs suspensions were shaken on thermostated shaker at 150 rpm for 2 h. After adsorption experiments, the 50 ml centrifuge tubes were centrifuged at 12,000 rpm (5810R, Eppendorf, Germany) for 4 min, and the supernatant solutions were pipetted from the centrifuge tubes. The supernatant solutions were pipetted from the centrifuge tubes and filtered through disposable 0.45 mm pore size polycarbonate filter. The conditions affecting Cd adsorption onto TNPs or HA–TNPs were also studied by systematically varying the pH and temperature. The Cd concentrations in the equilibrium aqueous phase were determined by graphite furnace atomic absorption spectrometry (AA-600, Perkin- Elmer, USA). The percent of removed Cd by the adsorbents was calculated by the following formula:

$$\%\ Removal = \frac{(C_0 - C_e)}{C_0} \times 100 \quad (1)$$

The adsorption capacity of Cd was calculated from the following mass balance equation:

$$q_e = \frac{(C_0 - c_e)V}{m} \quad (2)$$

where q_e (μg g^{-1}) is the equilibrium adsorption capacity; C_0 and C_e (μg L^{-1}) are the initial and equilibrium concentrations of Cd in solution; V (L) is the volume of aqueous solution containing Cd; and m (g) is the weight of adsorbent. The experiments were performed in triplicate and mean values were taken into account. The relative deviations met with the requirement of less than 5%.

2.4. Desorption and reusability studies

To examine the usability of the adsorbent, the desorption behavior of HA–TNPs was investigated. For desorption studies, were carried out in 5 mL of 0.05 N H_2SO_4 maintained at a constant temperature of 298 K. The Cd adsorbed HA–TNPs were placed in the desorbing medium on a rotary shaker at 150 rpm for 30 min. The residual Cd in the solution was measured after HA–TNPs removal in order to estimate the amount of Cd desorbed.

Reusability study of HA–TNPs was carried out by following the adsorption–desorption study for 5 cycles. The adsorption efficiency in each cycle was analyzed. Both the adsorption and desorption experiments were followed as described above.

3. Results and discussion

3.1. Adsorbent characterization

The characterization results FTIR of TNPs and HA–TNPs with different concentrations of HA are shown in Fig. 1. The data show that observed peak of TNPs at 1627 cm^{-1} shifted to 1617 cm^{-1}, 1615 cm^{-1} and 1622 cm^{-1} for 100–HA–TNPs, 250–HA–TNPs, and 350–HA–TNPs respectively. As exposed in Fig. 1, absorption spectra suggest strong interactions of phenolic OH of HA with TNPs. These shifts in characteristic wave numbers in the direction of lower wave numbers, indicated the presence of strong hydrogen bonds between the –OH groups and also between the –C=O– groups [41]. Surprisingly, 250–HA–TNPs showed the largest shift as well as strongest absorbance. This may be due to ligand exchange between TNPs and HA and larger band gap as shown in Fig. 2B. In comparison with pure TNPs, a number of continu-

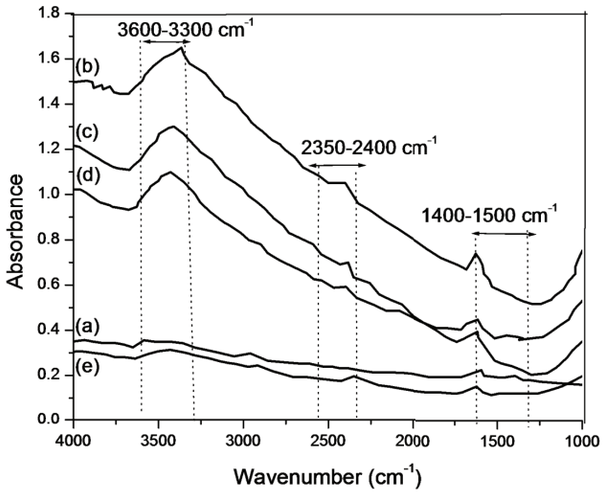

Fig. 1. FTIR spectra of HA (a) TNPs (b) adsorbed 100 – HA on TNPs (c) adsorbed 250 – HA on TNPs (d) adsorbed 350 – HA on TNPs (e).

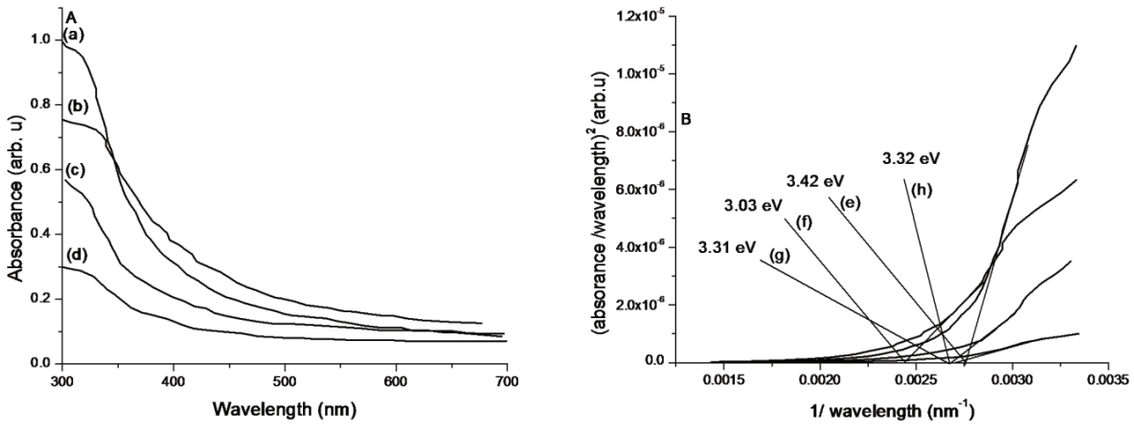

Fig. 2. Light absorbance A (a,b,c,d) and band gap energy B (e,f,g,h) of TNPs, 100 – HA – TNPs, 250 – HA – TNPs, 350 – HA –TNPs respectively.

ous new peaks around 1400–1500 cm^{-1} showed after binding with HA, owing c=c and C=O stretch of HA, particularly, the tiny peak around 1320, 1345 and 1530 cm^{-1} should be Vs_{C-O}, Vas_{C00-}, and Vs_{COO-}. Furthermore, the peak of O – H stretching bond at 3300–3600 cm^{-1} may appear from a various extent of ligand exchange between phenolic groups in TNPs and HA. We also observed that as amount of HA increased the peak at 2350–2400 becomes weaker, owing to the strong interactions of phenolic groups with TNPs. Compared with the ones coated with HA at 250 and 100 mg L^{-1}, there is sharp increase in intensity of the peak of the O–H, around 3500 cm^{-1}, in TNPs after modifying with HA at 350 mg L^{-1}. This could happen as a consequence of the ligand exchange between –OH groups and TNPs and HA carboxyl/hydroxyl functional groups [38]. FTIR analyses demonstrated the successful modification of TNPs surface with HA.

Fundamental absorption in a material corresponds to movement of electron from valence band to conduction band; this information is useful in determining band gap of material. The UV–visible spectra of the sampled nanoparticles are exposed in Fig. 2A. It is observed that modified the TNPs with HA resulted in an increased in photon absorbance. The optical band gap was determined via method described by Ghobadi [42]. We have plotted $(A/\lambda)^2$ as function of $1/\lambda$, where, A is the absorbance and λ is the wavelength. This plot gave a typical graph consisting of a linear portion, as shown in Fig. 2B. The optical band gap was determined by extra plotting the linear portion of the plot to $(A/\lambda)^2 = 0$ (to intercept the x-axis). The band gap of TNPs (E_g = 3.42 eV) is higher than that reported in the literature (E_g = 3.0 eV for rutile and around 3.2–3.25 eV for anatase titania) [43]. The HA coated TNPs revealed new deep levels which are at 3.03, 3.31 and 3.32, for 100 – HA – TNPs, 250 – HA – TNPs, and 350 – HA – TNPs, respectively. Interestingly, it is found that the HA coating changed the band gap property of TNPs. Similar conclusion was found on fabrication of methylammonium lead iodide ($CH_3NH_3PbI_3$) films from different molar ratios of CH_3NH_3I to PbI_2, the optical band gap of $CH_3NH_3PbI_3$, tuned from 1.52 eV to 2.64 eV by varying the CH_3NH_3I concentration [44]. However this was attributed that the HA coating can reduce the adhesion of TNPs that will be explained in the following section.

Table 1
Organic carbon contents and band gap energy of TNPs and HA – TNPs

Material type	*C*, (%)	C_e, (mg TOC L^{-1})	E_g (eV), Exp
TNPs	0.032	Undetectable	3.42
100 – HA – TNPs	0.938	2.40	3.03
250 – HA – TNPs	2.306	4.60	3.31
350 – HA – TNPs	2.355	56.40	3.32

[a]C: organic carbon content, representing adsorbed HA amount for coated TNPs: C_e: residual HA concentrations in solution after coating; E_g: band energy gap of TNPs and HA – TNPs.

Based on the TOC measurement showed that the amount of HA coated on 100 – HA – TNPs, 250 – HA – TNPs, and 350 – HA – TNPs was 0.938%, 2.306% and 2.355%, respectively in terms of carbon content as shown in Table 1. The linear increase of the coating percentage from 100 – HA to250 – HA implied that HA coating on TNPs processed with multilayer formation. In contrast, the data indicated that there was no significant difference between the HA coated TNPs prepared at 250 and 350 mg L^{-1} as shown in Table 1. This verifies the previous result which indicates chemical adhesion for TNPs reduced due to narrow band gap energies 3.31 and 3.32 eV for 250 – HA – TNPs, and 350 – HA – TNPs, respectively. Therefore, we select 350 mg L^{-1} HA coating from further analysis and testing.

3.2. Adsorption kinetics

Kinetics adsorption of Cd onto TNPs and HA–TNPs are shown in Fig. 3. A rapid adsorption of Cd occurred within 100 min, and then followed by a slow adsorption until the adsorbed Cd finally achieved a plateau value after 2 h which might be because of vacant adsorption spots decrease as the adsorbent becomes covered [45]. Kinetic study was significant to an adsorption process because it illustrated the elimination rate of Cd, and controlled the

residual time of the whole adsorption process. To well understand the adsorption mechanism and kinetics, two kinetic models including pseudo-first-order and pseudo-second-order were preferred to examine the kinetics of Cd adsorption onto TNPs and HA–TNPs. The pseudo-first-order kinetic model [46] and pseudo-second-order model [47] are presented as follows:

$$\text{Log}\,(q_e - q_t) = \log q_e - (k_1/2.303)t \quad (3)$$

$$t/q_t = 1/k_2\, q_e^2 + (1/q_e)t \quad (4)$$

where q_e and q_t are the amount of Cd adsorbed for adsorbent (μg g^{-1}) at equilibrium and at time t, respectively; k_1(min^{-1}) and k_2 (g(μg $min)^{-1}$) are the rate constant of pseudo-first-order kinetic model and pseudo-second-order model rate constant, respectively. The values of k_1 and q_e for Cd adsorption by TNPs and HA–TNPs were determined from the plot of log $(q_e - q_t)$ vs. t (Fig. 3B). The plots of t/q_t versus t based on the pseudo-second-order kinetic are shown in Fig. 3C.

Table 2 illustrates the predicted model constants of the above two equations. It was observed that the correlation coefficients (r^2) values for the pseudo-first-order kinetic model were relatively low and the calculated q_e values did not agree with the experimental ones. This showed that the pseudo-first-order kinetic model could not sufficiently illustrate the adsorption of Cd onto TNPs and HA–TNPs. Actually; in majority cases researchers have found the pseudo-first-order equation does not fit well to the whole range of contact time and is commonly valid over the initial stage of the adsorption processes [48]. For the pseudo-second-order kinetic model, the calculated correlation coefficient (r^2) was closer to unity. Furthermore, the calculated q_e values agreed very well with the experimental ones, illustrate a good linearity with r^2 above 0.99. As the experimental data were in good agreement with the pseudo-second-order model which suggested that the rate-limiting step in adsorption is controlled by chemical process [49]. It demonstrated that the Cd adsorption capacity was proportional to the number of active sites occupied on TNPs and HA–TNPs. As the adsorption process went on, active adsorption sites would decline. Therefore, the rate of the Cd adsorption by TNPs and HA–TNPs mostly depended on the available adsorption sites on TNPs and HA–TNPs for Cd at any time

3.3. Effect of pH onthe absorption of Cd

The effect of pH on the adsorption capacity at equilibrium conditions is shown in Fig.4A. The results indicate that the adsorption capacity of Cd onto TNPs and HA–TNPs increased slightly from pH 3.0 to 5.0, sky scraped from pH 5.0 to 8.0, and afterward researching a maximum at pH 8.0 to 10.0. Fig. 4E shows the Zeta potential curve of TNPs and HA–TNPs, it can be seen that the points of zero charge (PZC) locate at pH 4.2 and 3.9 for TNPs and HA–TNPs, respectively. When pH < pHpzc value, there would be a competition between protons and Cd ions in the adsorption on surface groups of HA–TNPs, resulting in low Cd adsorption. Furthermore, when the active sites are protonated, the surface of HA–TNPs becomes positively charged and consecutive adsorption of Cd ions in solution

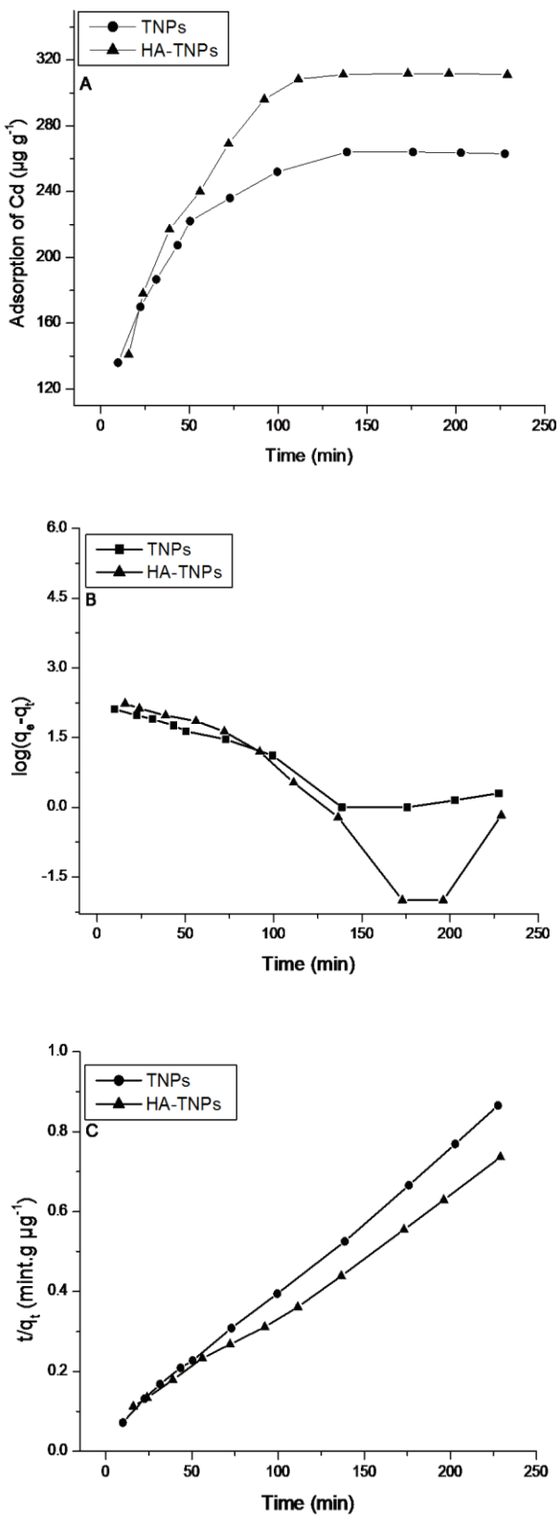

Fig. 3. Effect of contact time on adsorption capacity of Cd on TNPs and HA–TNPs (A); the fitting of different kinetic models for Cd adsorption onto TNPs and HA–TNPs; pseudo-first-order(B), pseudo-second-order(C). [Adsorption conditions: adsorbent dosage = 10 mg L^{-1}, pH 7.0, and temperature = 298 K].

Table 2
Pseudo-first-order and pseudo-second-order kinetic model constants for Cd adsorption onto TNPs and HA–TNPs

Fitting model	Adsorbents	$q_{e'}$ (μg g^{-1}), exp	$q_{e'}$ (μg g^{-1}), cal	K_1, (min^{-1})	r^2
Pseudo-first- order mode	TNPs	265.00	138.12	2.387-E02	0.875
	HA–TNPs	311.68	0.045	4.415-E02	0.780
	Adsorbents	q_e (μg g^{-1}), exp	q_e (μg g^{-1}), cal	K_2 (g(μg mint)$^{-1}$)	r^2
Pseudo-second-order model	TNPs	265.00	284.20	2.460-E04	0.999
	HA–TNPs	311.68	349.16	1.326-E04	0.996

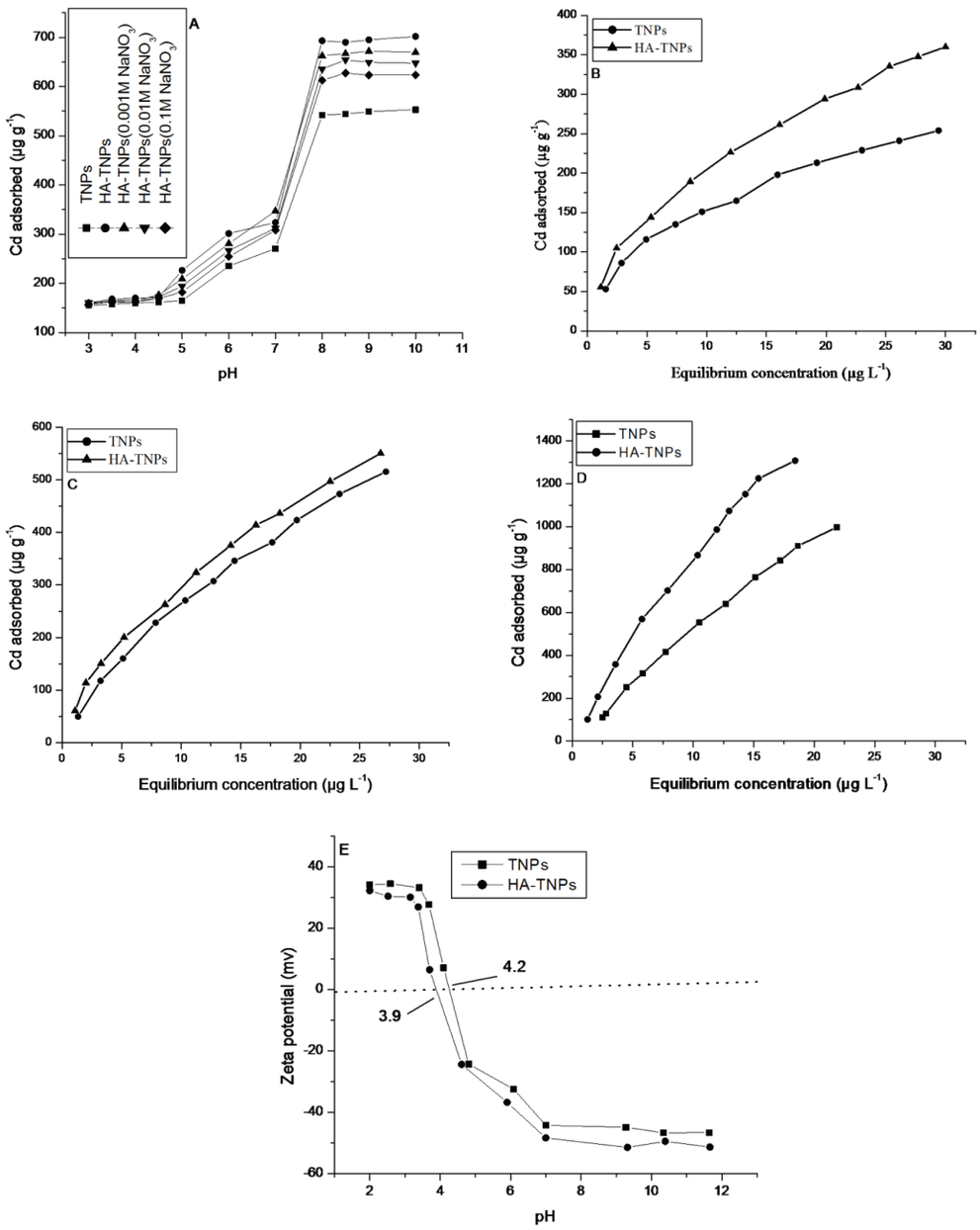

Fig. 4. Effect of pH, ionic strength on the adsorption of Cd onto TNPs and HA–TNPs (A) and Freundlich adsorption curves of Cd onto TNPs and HA–TNPs at various pH. 5.0 (B), 7.0 (C) and 10.0 (D). Zeta potential of TNPs and HA–TNPs at different pH (E). [Adsorption conditions: adsorbent dosage = 10 mg L^{-1}, and temperature = 298 K].

on the surface is less probable to occur. Regarding the point of zero charge (pHpzc) of HA–TNPs, in solution having pH value lower than pHpzc of HA–TNPs, the surface sites could be protonated and positively charged. Alternatively, the active sites are deprotonated when the solution pH is higher than pHpzc, resulting in negatively charged sites and the adsorption of Cd cations on HA–TNPs could possibly take place via electrostatic interaction with the negatively charged sites on HA–TNPs. However, in this study, the maximum adsorption of Cd was observed at pH values near or above than pH_{PZC} of adsorbents (pH_{pzc} TiO_2= 4.2, pH_{pzc}HA = 1.9). This may be due to the development of negative charge on the surface of the adsorbents. Therefore, the parts of adsorption of Cd ions on HA–TNPs surface for Cd would occur via electrostatic interaction. It was observed that that HA aliphatic chains are the basic structure for HA fractions on HA–TNPs [50], and they might form net, stretch, or spongy structures below pH 7.0, but condensed when solution pH is above 7.0 [51]. Therefore, more available adsorption sites would be exposed for Cd with pH increase. Meanwhile, the complexation effect for Cd would weaken.

Therefore, Cd adsorption was investigated using the Langmuir model and the Freundlich model, which are presented as follows:

$$\text{Log } q_e = \log k_F + 1/n \log C_e \quad (5)$$

$$C_e/q_e = C_e/q_m + 1/q_m K_L \quad (6)$$

where q_m and C_e are the amount of metal adsorbed (μg g^{-1}) and the equilibrium metal concentration (μg L^{-1}), respectively. k and n are the Freundlich constants which are related to adsorption capacity and intensity, respectively. Adsorption isotherms parameters and correlation coefficients (r^2) of Cd on TNPs and HA–TNPs at pH 5.0, 7.0, and 10.0 calculated from Freundlich and Langmuir adsorption model as shown in Table 3. The Freundlich model is found to be the best fit with the test data, with the highest correlating coefficient (r^2) as shown in Table 3. n is a dimensionless parameter correlated to the surface heterogeneity, and if the value of n approaches 1, it is represented of homogeneous surface [52]. n values of Freundlich parameter of Cd adsorption on TNPs and HA–TNPs were both near 1, which demonstrated that both adsorbents possessed relative homogeneous surfaces. While K_F value of Freundlich adsorption coefficient is a unit-capacity parameter, defined as the concentration adsorbed per gram of the adsorbent divided by its equilibrium concentration C_e, a higher K_F shows a higher selectivity or adsorption. K_F (HA–TNPs) were higher than the corresponding K_F (TNPs) at pH 5.0, 7.0 and 10.0, suggesting that the adsorption capacity of HA–TNPs was stronger than TNPs.

The adsorption capacity of the HA–TNPs particles from the Langmuir isotherm is 813 μg g^{-1}. This value is higher than the reported 52.5, 500 and 700 μg g^{-1} of Cd adsorption on Arsenic (As) and selenium (Se) ion imprinted polymers [53], TiO_2 (degussa P 25) [54], and commercially activated carbon adsorbents, respectively [55] and comparable to the 1390 μg g^{-1} adsorption capacity of Cd on a commercially available Granular activated carbon [56].

3.4.. Effect of ionic strength on the Cd absorption

The ionic strengths of 0.1 mM, 0.01 mM and 0.001 mM $NaNO_3$ were chosen to examine their effect on Cd adsorptions onto HA–TNPs. Fig. 4A shows that Cd adsorption decreased with increasing ionic strength (Na ions concentration in solution). With increasing Na ions concentration in solution, the competitive adsorption of Cd with the Na ions adsorbed on Na–HA–TNPs surface increases and thereby the adsorption of Cd on Na–HA–TNPs decreases. This phenomenon could be attributed to two reasons: Firstly, a decreasing electrolyte concentration favored the complexation tendency of Cd ions with the hydroxyl functional groups on HA–TNPs, which increases the adsorption process. Secondly, an increasing ionic strength of solution influenced the activity coefficient of metal ions that may have limited their transfer to the surfaces [57].

Table 3
Predicted isothermal constants of Cd by Freundlich and Langmuir isotherms at different pH

Model type	pH	Adsorbents	K_F ((μg g^{-1}·(L $μg^{-1}$)$^{-n}$)	$1/n$	r^2
Freundlich adsorption	5	TNPs	47.915	0.502	0.994
		HA–TNPs	56.569	0.551	0.993
	7	TNPs	44.882	0.756	0.993
		HA–TNPs	68.133	0.638	0.993
	10	TNPs	50.396	0.996	0.989
		HA–TNPs	97.469	0.933	0.987
	pH	Adsorbents	q_m (μg g^{-1})	K_L (L $μg^{-1}$)	r^2
Langmuir adsorption	5	TNPs	3.17E+02	0.110	0.981
		HA–TNPs	4.68E+02	0.092	0.972
	7	TNPs	9.64E+02	0.039	0.976
		HA–TNPs	8.13E+02	0.066	0.957
	10	TNPs	3.21E+04	0.002	0.019
		HA– TNPs	6.35E+03	0.015	0.524

3.5. Effect of competing cations on the Cd adsorption

In order to examine the influence of competing cations on Cd adsorption, the adsorption of Cd on HA–TNPs was investigated in 0.001–0.01 mmol L^{-1} KNO_3, 10–50 μg L^{-1} $Ca(NO_3)_2$, and 10–50 μg L^{-1} $Pb(NO_3)_2$, respectively. All the interfering cation solutions were prepared from their nitrate salts, as nitrate anions were thought not to play a part in adsorption, forming only weak complexes with metals. Fig. 5 illustrates that the Cd adsorption capacity decreased at different degrees in the presence of competing cations. The influence sequence of coexisting cations on adsorption of Cd to HA–TNPs was in the range of $Pb^{2+} > Ca^{2+} > K^+$. It seemed that the presence of appreciable quantities of K^+ had no obvious effects on Cd adsorption. This behavior might be attributed to the fact that K^+ ion had poor affinity towards the adsorption sites of HA–TNPs compared with Cd. As shown in Fig. 5, it was obvious that the presence of Pb^{2+} in solution significantly reduced Cd adsorption; the higher the Pb^{2+} concentration, the more pronounced efficiency reduction in Cd removal. A similar effect was found for Ca^{2+}. It was considered that the binding sites on HA–TNPs surface were limited and when other cations, such as Ca^{2+}, Pb^{2+} were present in Cd solution, they were also adsorbed onto HA–TNPs surface in addition to Cd. The effective binding sites available for Cd adsorption thus reduced, depending on the equilibria between adsorption competitions from all the cations. The results in Fig. 5 also showed that different cations had different affinities to the HA–TNPs binding sites; hence, Cd adsorption inhibited to varying degrees. It was showed that Pb^{2+} inhibited Cd adsorption more significantly than Ca^{2+}. This could be elucidated that the stronger surface complexation of Pb^{2+} with carboxyl and/or phenolic groups in HA than Ca^{2+}.

3.6. Effect of temperature on the adsorption of Cd

To observe the effect of temperature, adsorption studies of Cd onto TNPs and HA–TNPs were performed at three different temperatures: 298, 315, 313 K as shown in Fig. 6. The data of the Cd adsorbed at equilibrium (q_e, μg g^{-1}) and the equilibrium Cd concentration (C_e, μg L^{-1}) were fitted to the Langmuir and Freundlich adsorption model in Eqs. (5) and (6). Adsorption parameters and correlation coefficients (r^2) of Langmuir and Freundlich adsorption model is listed in Table 4. As Table 4 shows, both the models adequately predicted adsorption of Cd on HA–TNPs, however; only the Freundlich equation yielded a better fit. This suggests that HA–TNPs have characteristics with several possible functional groups responsible for adsorption of Cd. In addition, the parameter *k* of Freundlich model increased as the temperature enhanced, so did the adsorption amount of Cd. The adsorption capacity significantly increased by 34%, 50% and 59% at 298, 315 and 332 K, respectively for Cd based on their respective Freundlich k values. The increase in metal uptake with increasing temperature may be due to either higher affinity of sites for Cd or an increase in the number of binding sited on HA–TNPs.

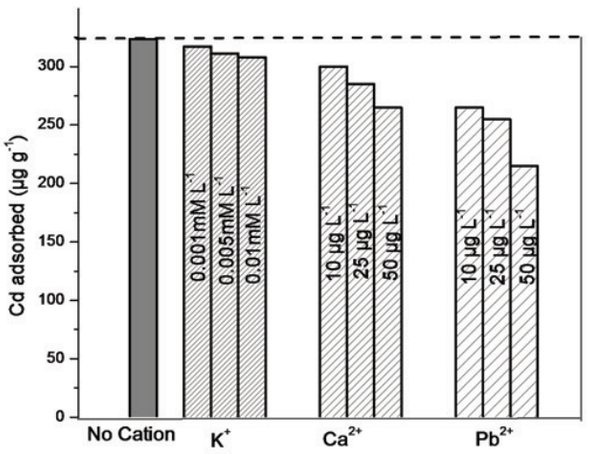

Fig. 5. Effects of competing cations on the adsorption of Cd by HA–TNPs.

This high adsorption capacity exhibited by HA–TNPs-may be explained by its nano-scale particle size giving access to a larger surface area as well as the incorporation of a large number of hydroxyl functional groups of HA, which provided effective adsorption sites for the binding of Cd [28–30]. Table 4 as well as Fig. 6 amply demonstrates the sensitivity of the adsorption process towards temperature and it is observed that adsorption increases with increase in temperature for all cases.

3.7. Thermodynamic study

To further estimate the effect of temperature on the adsorption and examine the possible mechanism involved in the adsorption process, the thermodynamic behaviors were calculated as follows. The free energy of adsorption process, considering the adsorption equilibrium coefficient K_0, is given by the equation:

$$\Delta G^\circ = -RT \ln K_0 \quad (7)$$

where ΔG^0 is the standard free energy of adsorption (kJ mol^{-1}), T is the temperature in Kelvin and R is the universal gas constant (8.314 J $(mol\ K)^{-1}$). The adsorption distribution coefficient K_0, was determined from the slope of the plot ln q_e/C_e against q_e at different temperatures and extrapolating to zero q_e according to the method suggested by Khan and Singh [58]. The values of enthalpy change (ΔH°) and entropy change (ΔS°) were calculated from the slope and intercept of the plot of ΔG° vs. T , using the equation:

$$\Delta G^\circ = \Delta H^\circ - T\,\Delta S^\circ \quad (8)$$

Table 5 which summarizes the values of these parameters demonstrates the endothermic nature of the adsorption process (ΔH° values are positive). A possible explanation is that Cd ions are well hydrated and will require breaking of the hydration sheath so as to proceed for adsorption; this in turn requires high energy. High temperature hence favors the dehydration process and ultimately the adsorption phenomenon too. Similar observation and explanation have been given [59].

The negative ΔG°value suggests that the adsorption process is a spontaneous process and thermodynamically favorable under the experimental conditions. The decrease of ΔG° with increasing temperature indicates more efficient adsorption at higher temperature. In addition, at higher temperature,

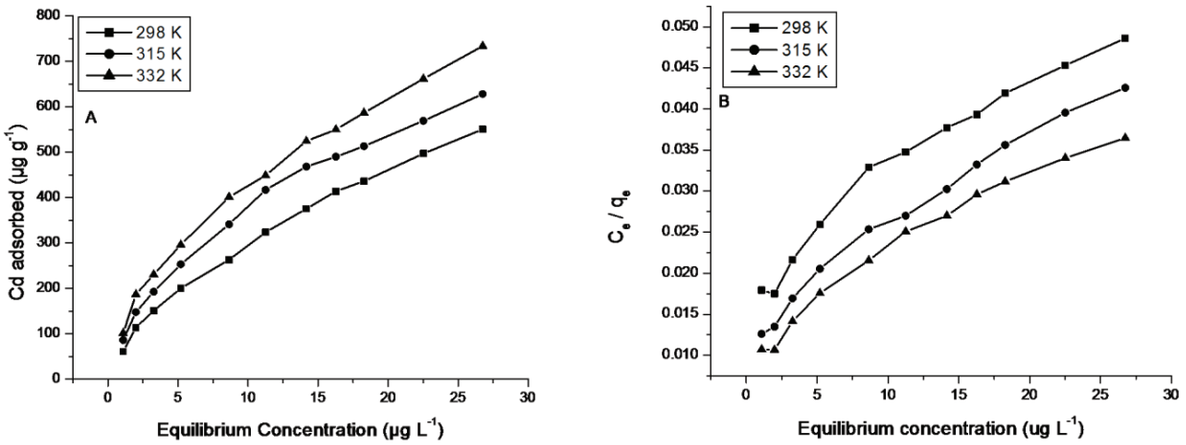

Fig. 6. Langmuir and Freundlich isotherms at different temperatures for the adsorption of Cd onto TNPs and HA–TNPs). [Adsorption conditions: adsorbent dosage = 10 mg L^{-1}, pH 7.0].

Table 4
Predicted isothermal constants of Cd by Freundlich and Langmuir isotherms at different temperatures

Model type	Parameter	Temperature (K)		
		298	315	332
Freundlich adsorption	K_F (µg g^{-1}.(L µg^{-1})$^{-n}$)	68.133	91.385	110.936
	$1/n$	0.638	0.602	0.581
	r^2	0.993	0.993	0.990
Langmuir adsorption	q_m (µg g^{-1})	813.347	862.420	972.409
	K_L (L µg^{-1})	0.066	0.087	0.090
	r^2	0.957	0.981	0.966

Table 5
Thermodynamic parameters of the Cd adsorption onto HA–TNPs at different temperatures

Temperature (K)	ln K_0	ΔG^0 (kJ mol^{-1})	ΔH^0 (kJ mol^{-1})	ΔS^0 (J mol^{-1} K^{-1})
298	4.131	–9.721		
315	4.522	–11.202	15.351	88.691
332	4.762	12.393		

the Cd are readily desolvated, which enhances the sorption process. The positive ΔS° values indicate the affinity of the adsorbents towards Cd in aqueous solutions and may suggest increasing degree of freedom at the solid–liquid interface during the sorption of metal ions on to the adsorbents [50].

3.8. Desorption and reusability studies

Desorption of the loaded adsorbent is a key factor for improving the economies of the adsorption process, and to some extent can clear the mechanism of the sorption. Desorption experiments carried out with Cd laden HA–TNPsin 0.05 N H_2SO_4 showed that approximately 88% of the adsorbed

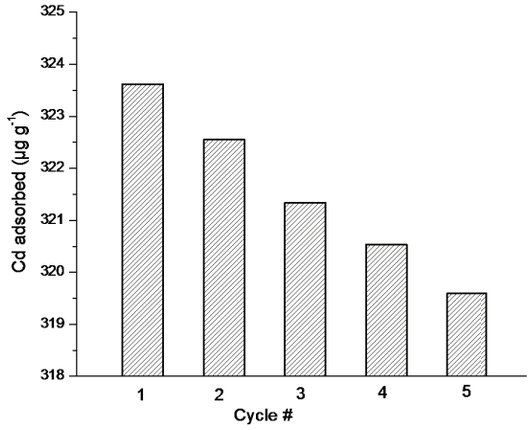

Fig. 7. Recycling of HA–TNPs in the removal of Cd [average value of 3 tests, error < 2.32%].

cadmium was desorbed. Results of the adsorption capacity of HA–TNPs for five consecutive adsorption–desorption cycles are graphically illustrated in Fig. 7. In all cycles, desorption was 88.27–88.33%. Therefore, we concluded that the physically adsorbed cadmium was desorbed at the fifth cycle. We also attributed the dissolution of $Cd(OH)_2$ to both electrostatic and complexation reactions occurring between the HA–TNPs and the Cd ions, which prevented complete desorption. A 1.24 % decrease in adsorption efficiency occurred after five consecutive cycles of adsorption–desorption that demonstrates good stability and reusable properties in the studied experimental conditions [Fig. 7]. This fulfills an important criterion for advanced adsorbents.

4. Conclusions

This study focused on assessing the adsorption efficiency of a novel HA–TNPs adsorbent synthesized from a natural organic matter for a toxic Cd metal ion. The modifying characterations have been confirmed by FTIR and

UV–visible spectrophotometer. The HA–TNPs adsorbent could successfully be utilized to remove Cd from aqueous media. The solution pH and temperature greatly affected the adsorption of Cd onto HA–TNPs. The adsorption kinetics for the removal of Cd by TNPs and HA–TNPs was well elucidated by pseudo-second-order kinetic model which suggested that the Cd uptake was a chemisorption process. The equilibrium data could be well explained by the Freundlich isotherms. The partition distribution coefficient (k) of HA–TNPs increased by 34%, 50% and 59% for Cd at 298, 315 and 332 K, respectively as compared to the bare TNPs, which could be attributed that HA–TNPs has a stronger affinity of sites for Cd adsorption than that of bare TNPs. These findings indicates that HA modification being a useful method to improve the adsorption affinity of metallic contaminants onto TNPs. Thermodynamic calculations demonstrates that the Cd adsorption process by HA–TNPs was spontaneous, endothermic and entropy-increasing in nature. Results of this study were of great significance for environmental applications of modified TNPs nanoparticles as a promising candidate material for Cd removal from aqueous media.

Acknowledgments

This work was supported by the National Natural Science Foundation of China (41571315), CAS President's International Fellowship Initiative China (2017PCOO59) and key project of China National Tobacco corporation Sichuan (SCYC 201504).

References

[1] J.F. Liu, Z.S. Zhao, G.B. Jiang, Coating Fe_3O_4 magnetic nanoparticles with humic acid for high efficient removal of heavy metals in water, Environ. Sci. Technol., 42 (2008) 6949–6954.

[2] A.R. Contreras, A. García, E. González, E. Casals, V. Puntes, A. Sánchez, X. Font, S. Recillas, Potential use of CeO_2, TiO_2 and Fe_3O_4 nanoparticles for the removal of cadmium from water, Desal. Water Treat., 41 (2012) 296–300.

[3] M. Wu, T. Duan, Y. Chen, Q. Wen, Y. Wang, H. Xin, Surface modification of TiO_2 nanotube arrays with metal copper particle for high efficient photocatalytic reduction of Cr(VI), Desal. Water Treat., 57 (2016) 10790–10801.

[4] Ş. Akkan, İ. Altın, M. Koç, M. Sökmen, TiO_2 immobilized PCL for photocatalytic removal of hexavalent chromium from water, Desalin. Water Treat., 56 (2014) 2522–2531.

[5] S. Mahdavi, J. Mohsen, A. Abbas, Heavy metals removal from aqueous solutions using TiO_2, MgO, and Al_2O_3 nanoparticles, Chem. Eng. Commun., 200 (2013) 448–470.

[6] M. Inyang, B. Gao, Y. Yao, Y. Xue, A.R. Zimmerman, P. Pullammanappallil, X. Cao, Removal of heavy metals from aqueous solution by biochars derived from anaerobically digested biomass, Bioresour. Technol., 110 (2012) 50–56.

[7] A. Kaur, U. Gupt, A review on applications of nanoparticles for the preconcentration of environmental pollutants, J. Mater. Chem., 19 (2009) 8279–8289.

[8] Y.H. Li, J. Ding, Z.K. Luan, Z.C. Di, Y.F. Zhu, C.L. Xu, D.H. Wu, B.Q. Wei, Competitive adsorption of Pb^{2+}, $Cu^{2+}$and Cd^{2+} ions from aqueous solutions by multiwalled carbon nanotubes, Carbon, 41 (2003) 2787–2792.

[9] D. Karabelli, C.¨Uz¨um, T. Shahwan, A.E. Eroglu, T.B. Scott, K.R. Hallam, I. Lieberwirth, Batch removal of aqueous Cu^{2+} ions using nanoparticles of zero-valent iron: a study of the capacity and mechanism of uptake, Ind. Eng. Chem. Res., 47 (2008) 4758–4764.

[10] O.A. Dada, F.A. Adekola, E.O. Odebunmi, Kinetics and equilibrium models for sorption of Cu(II) onto a novel manganese nano-adsorbent, J. Dispersion Sci. Technol., (2015), http://dx.doi.org/10.1080/01932691.2015.1034361.

[11] Y.H. Chen, F.A. Li, Kinetic study on removal of copper(II) using goethite and hematite nano-photocatalysts, J. Colloid Interface Sci., 347 (2010) 277–281.

[12] N.C. Feitoza, T.D. Goncalves, J.J. Mesquita, J.S. Menegucci, M.K.M.S. Santos, J.A. Chaker, R.B. Cunha, A.M.M. Medeiros, J.C. Rubim, M.H. Sousa, Fabrication of glycine-functionalized maghemite nanoparticles for magnetic removal of copper from wastewater, J. Hazard. Mater., 264 (2014) 153–160.

[13] L. Yang, Z. Wei, W. Zhong, J. Cui, W. Wei, Modifying hydroxyapatite nanoparticles with humic acid for highly efficient removal of Cu(II) from aqueous solution, Colloids Surf. A., 490 (2016) 9–21.

[14] X. Qu, P.J.J. Alvarez, Q. Li, Applications of nanotechnology in water and wastewater treatment, Water Res., 47 (2013) 3931–3946.

[15] J. Wang, L. Wang, Y. Fan, Adverse biological effect of TiO_2 and hydroxyapatite nanoparticles used in bone repair and replacement, Int. J. Mol. Sci., 17 (2016) 1–14.

[16] K.E. Engates, H.J. Shipley, Adsorption of Pb, Cd, Cu, Zn, and Ni to titanium dioxide nanoparticles: effect of particle size, solid concentration, and exhaustion, Environ. Sci. Pollut. Res., 18 (2011) 386–395.

[17] H. Jean-Marie, Photocatalysis fundamentals revisited to avoid several misconceptions, Appl. Catal. B, 99 (2010) 461–468.

[18] U.I. Gaya, A.H. Abdullah, Heterogeneous photocatalytic degradation of organic contaminants over titanium dioxide: A review of fundamentals, progress and problems, J. Photochem. Photobiol. C, 9 (2008) 1–12.

[19] J.L. Blin, M.J. Stébé, T. Roques-Carmes, Use of ordered mesoporous titania with semi-crystalline framework as photocatalyst, Colloids Surf. A, 407 (2012) 177–185.

[20] M. Kassir, T. Roques-Carmes, T. Hamieh, J. Toufaily, M. Akil, O. Barres, F. Villiéras, Improvement of the photocatalytic activity of TiO_2 induced by organicpollutant enrichment at the surface of the organografted catalyst, Colloids Surf. A, 485 (2015) 73–83.

[21] P. Dutta, A. Ray, V. Sharma, J. Millero, Adsorption of arsenate and arsenite on titanium dioxide suspensions, J. Colloid Interface Sci., 278 (2004) 270–275.

[22] Z. Xu, X. Liu, Y. Ma, H. Gao, Interaction of nano-TiO_2 with lysozyme: insights into the enzyme toxicity of nanosized particles, Environ. Sci. Pollut. Res., 17 (2010) 798–806.

[23] G.W. Stephen, H. Li, H. Jennifer, C. Da-Ren, K. In-Chul, J.T. Yinjie, Phytotoxicity of metal oxide nanoparticles is related to both dissolved metals ions and adsorption of particles on seed surfaces, J. Pet. Environ. Biotechnol., 3 (2012) 4.

[24] A. Servin, W. Elmer, A. Mukherjee, D.T.R. Roberto, H. Hamdi, J.C. White, P. Bindraban, C. Dimkpa, A review of the use of engineered nanomaterials to suppress plant disease and enhance crop yield, J. Nanopart. Res., 17 (2015) 92.

[25] J. Hu, G. Chen, I.M.C. Lo, Removal and recovery of Cr(VI) from wastewater by maghaemite nanoparticles, Water Res., 39 (2005) 4528–4536.

[26] Y.F. Shen, J. Tang, Z.H. Nie, Y.D. Wang, Y. Ren, L. Zuo, Preparation and application of magnetic Fe_3O_4 nanoparticles for wastewater purification, Sep. Sci. Technol., 68 (2009) 312–319.

[27] S.H. Huang, D.H. Chen, Rapid removal of heavy metal cations and anions from aqueous solutions by an amino-functionalized magnetic nano-adsorbent, J. Hazard. Mater., 163 (2009) 174–179.

[28] S.S. Banerjee, D.H. Chen, Fast removal of copper ions by gum arabic modified magnetic nano-adsorbent, J. Hazard. Mater., 147 (2007) 792–799.

[29] Y.C. Chang, D.H. Chen, Preparation and adsorption properties of monodisperse chitosan-bound Fe_3O_4 magnetic nanoparticles for removal of Cu(II) ions, J. Colloid Interface Sci., 283 (2005) 446–451.

[30] A.Z.M. Badruddoza, A.S.H. Tay, P.Y. Tan, K. Hidajat, M.S. Uddin, Carboxymethyl-β -cyclodextrin conjugated magnetic nanoparticles as nano-adsorbents for removal of copper ions: synthesis and adsorption studies, J. Hazard. Mater., 185 (2011) 1177–1186.
[31] S.S. Shenvi, A.M. Isloor, A.F. Ismail, S.J. Shilton, A.A. Ahmed, Humic acid basedbiopolymeric membrane for effective removal of methylene blue andrhodamine B, Ind. Eng. Chem. Res., 54 (2015) 4965–4975.
[32] D.X. Li, C.F. Li, A.H. Wang, Q. He, J.B. Li, Hierarchical gold/copolymernanostructures as hydrophobic nanotanks for drug encapsulation, J. Mater. Chem., 20 (2010) 7782–7787.
[33] J.J. Lu, Y. Li, X.M. Yan, B.Y. Shi, D.S. Wang, H.X. Tang, Sorption of atrazine onto humic acids (HAs) coated nanoparticles, Colloids Surf. A: Physicochem. Eng. Aspects, 347 (2009) 90–96.
[34] S. Khan, H. Şengül, Experimental investigation of stability and transport of TiO_2 nanoparticles in real soil columns, Desal. Water Treat., 57 (2016) 26196–26203.
[35] W. Jiang, Q. Cai, W. Xu, M. Yang, Y. Cai, D.D. Dionysiou, K.E. O'shea, Cr(VI) adsorption and reduction by humic acid coated on magnetite, Environ. Sci. Technol., 48 (2014) 8078–8085.
[36] S. Yang, P. Zong, X. Ren, Q. Wang, X. Wang, Rapid and highly efficient preconcentration of Eu(III) by core–shell structured Fe_3O_4@humic acid magnetic nanoparticles, ACS Appl. Mater. Interfaces, 4 (2012) 6891–6900.
[37] J. Lua, Y. Li, X. Yan, B. Shi, D. Wang, H. Tang, Sorption of atrazine onto humicacids (HAs) coated nanoparticles, Colloids Surf. A, 347 (2009) 90–96.
[38] K. Yang, B.S. Xing, Sorption of phenanthrene by humic acid-coated nanosized TiO_2 and ZnO, Environ. Sci. Technol., 43 (2009) 1845–1851.
[39] Y. Sun, C. Chen, D. Shao, J. Li, X. Tan, G. Zhao, S. Yang, X. Wang, Enhanced adsorption of ionizable aromatic compounds on humic acid-coated carbonaceous adsorbents, RSC Adv., 2 (2012) 10359–10364.
[40] S. Mahdavi, A. Afkhami, H. Merrikhpour, Modified ZnO nanoparticles with new modifiers for the removal of heavy metals in water, Clean Technol. Environ. Policy, 17 (2015) 1645–1661.
[41] L .Stobinski, B. Lesiak, L. Kövér, J. Tóth, S. Biniak, G. Trykowski, J. Judek, Multiwall carbon nanotubes purification and oxidation by nitric acid studied by the FTIR and electron spectroscopy methods, J. Alloys and Compd., 501 (2010) 77–84.
[42] N. Ghobadi, Band gap determination using absorption spectrum fitting procedure, Int. Nano. Lett., 3 (2016) 2.
[43] J. Ananpattarachai, P. Kajitvichyanukul, S. Seraphin, Visible light absorption ability and photocatalytic oxidation activity of various interstitial N-doped TiO_2 prepared from different nitrogen dopants, J. Hazard. Mater., 168 (2009) 253–261.
[44] K. Xiaohan, Y. Jun, Z. Ao, Z. Bing, C. Yunlin, Optical band gap transition from direct to indirect induced by organic content of $CH_3NH_3PbI_3$ perovskite films, Appl. Phys. Lett., 107 (2015) 091904–4
[45] S. Khan., W. Yaoguo, Z. Xiaoyan, H. Sihai, L. Tao, F. Yilin, L. Qiuge, Influence of dissolved organic matter from corn straw on Zn and Cu sorption to Chinese loess, Toxicol. Environ. Chem., 95 (2013) 1318–1327.
[46] S. Lagergren, Zur theorie der sogenannten adsorption gelöster stoffe, K. Sven Vetenskapsakad. Handl., Band, 24 (1898) 1–39.
[47] G. McKay, Y.S. Ho, Pseudo-second order model for sorption processes, Process Biochem., 34 (1999) 451–465.
[48] W. Wei, L. Yang, W. Zhong, J. Cui, Z. Wei, Poorly crystalline hydroxyapatite: a novel adsorbent for enhanced fulvic acid removal from aqueous solution, Appl. Surface Sci., 332 (2015) 328–339.
[49] W. Wei, L. Yang, W. Zhong, J. Cui, Z. Wei, Mechanism of enhanced humic acid removal from aqueous solution using poorly crystalline hydroxyapatite nanoparticles, Digest J. Nanomat. Biostruct., 10 (2015) 663–680.
[50] X.J. Feng, A.J. Simpson, M.J. Simpson, Investigating the role of mineral-bound humic acid in phenanthrene sorption, Environ. Sci. Technol., 40 (2006) 3260–3266.
[51] Y. Chen, M. Schnitzer, Scanning electron microscopy of a humic acid and of a fulvic acid and its metal and clay complexes, Soil Sci. Soc. Am. J., 40 (1976) 682–686.
[52] Q. Chen, D. Yin, S. Zhu, X. Hu, Adsorption of cadmium(II) on humic acid coated titanium dioxide, J. Colloid Interface Sci., 367 (2012) 241–248.
[53] L.D. Mafu, B.B. Mamba, T.A.M. Msagati, Synthesis and characterization of ion imprinted polymeric adsorbents for the selective recognition and removal of arsenic and selenium in wastewater samples, J. Saudi. Chem. Soc., 20 (2016) 594–605.
[54] X. Xie, L. Gao, Effect of crystal structure on adsorption behaviors of nanosized TiO_2 for heavy-metal cations, Curr. Appl. Phys., 9 (2009) S185–S188.
[55] T.A.H. Nguyen, H.H. Ngo, W.S. Guo, J. Zhang, S. Liang, Q.Y. Yue, Q. Li, T.V. Nguyen, Applicability of agricultural waste and by-products for adsorptive removal of heavy metals from wastewater, Bioresour. Technol., 148 (2013) 574–585.
[56] T.K. Sen, M. Mohammod, S. Maitra, B.K. Dutta, Removal of cadmium from aqueous solution using castor seed hull: a kinetic and equilibrium study, Clean, 38 (2010) 850–858.
[57] C. Chen, J. Hu, D. Shao, J. Li, X. Wang, Adsorption behavior of multiwall carbon nanotube/iron oxide magnetic composites for Ni(II) and Sr(II), J. Hazard. Mater., 164 (2009) 923–928.
[58] A.A. Khan, R.P. Singh, Adsorption thermodynamics of carbofuran on Sn(IV)arsenosilicate in H^+, Na^+, and Ca^{2+} forms, Colloids Surf., 24 (1987) 33–42.
[59] C.L. Chen, X.K. Wang, Adsorption of Ni (II) from aqueous solution using oxidized multiwall carbon nanotubes, Ind. Eng. Chem. Res., 45 (2006) 9144–9149.